

## Supporting Information

### **Synthesis and Properties of Air-stable n-Channel Semiconductors Based on MEH-PPV Derivatives Containing Benzo[c]cinnoline Moieties**

**Jyh-Chien Chen,<sup>\*a</sup> Hsin-Chung Wu,<sup>a</sup> Chi-Jui Chiang,<sup>a</sup> Tuo Chen,<sup>a</sup> Li Xing<sup>b</sup>**

<sup>a</sup> Department of Materials Science and Engineering, National Taiwan University of Science and Technology, No. 43 Sec. 4 Keelung Rd., Taipei, 10607, Taiwan

<sup>b</sup> Pfizer Worldwide Research and Development, 200 Cambridge Park Drive, Cambridge, MA 02140, USA

Corresponding Author: Jyh-Chien Chen

Department of Materials Science and Engineering, National Taiwan University of Science and Technology, No. 43 Sec. 4 Keelung Rd., Taipei, 106, Taiwan

TEL: +886-2-27376526

FAX: +886-2-27376544

E-mail: [jcchen@mail.ntust.edu.tw](mailto:jcchen@mail.ntust.edu.tw)

## Structural Identification by NMR Spectroscopy

### Monomer

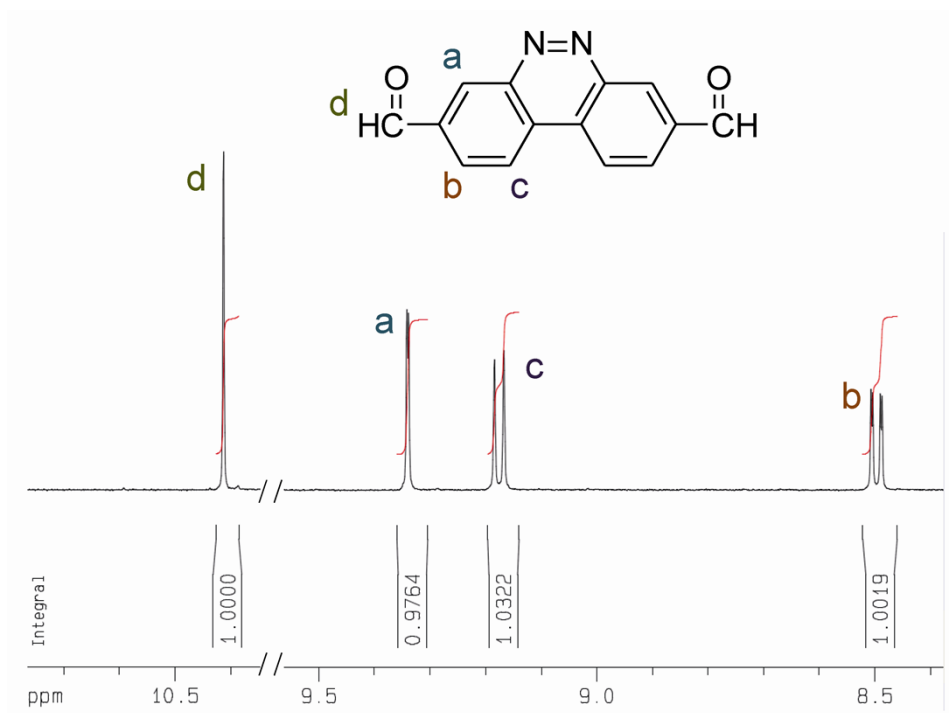


Fig. S1  $^1\text{H}$  NMR spectrum of compound **4** in  $\text{DMSO-}d_6$ .

### Polymers

Several *d*-solvents, such as  $\text{CDCl}_3$ ,  $\text{THF-}d_8$ , and  $\text{DMSO-}d_6$ , were used to prepare NMR samples. Quality NMR spectra can not be obtained due to the poor solubility except **P10** in  $\text{CDCl}_3$ . The  $^1\text{H}$  and  $^{13}\text{C}$  NMR spectra of **P10** in  $\text{CDCl}_3$  were shown in Fig. S2 and S3, respectively. Due to the limited solubility of **P10** in  $\text{CDCl}_3$ , these spectra were obtained after 128 scans ( $^1\text{H}$  NMR spectrum) and 18135 scans ( $^{13}\text{C}$  NMR spectrum). The peaks at 6.6~7.7 ppm in Fig. S2 were attributed to the hydrogens on vinylene linkages and phenyl rings of the MEH-PPV segments. The peaks of hydrogens on the benzo[*c*]cinnilone segments appeared at 8.77, 8.53, and 8.13 ppm. By comparing the  $^{13}\text{C}$  NMR spectra of MEH-PPV and **P10**, several new peaks appearing at 129.03, 128.22, and 125.29 ppm were assigned to the carbons on benzo[*c*]cinnoline segments (Fig. S3). The peaks of the quaternary carbons (B, E, and F in

Fig. S3) were too weak to be identified due to their nature and the limited solubility of **P10** in  $\text{CDCl}_3$ .

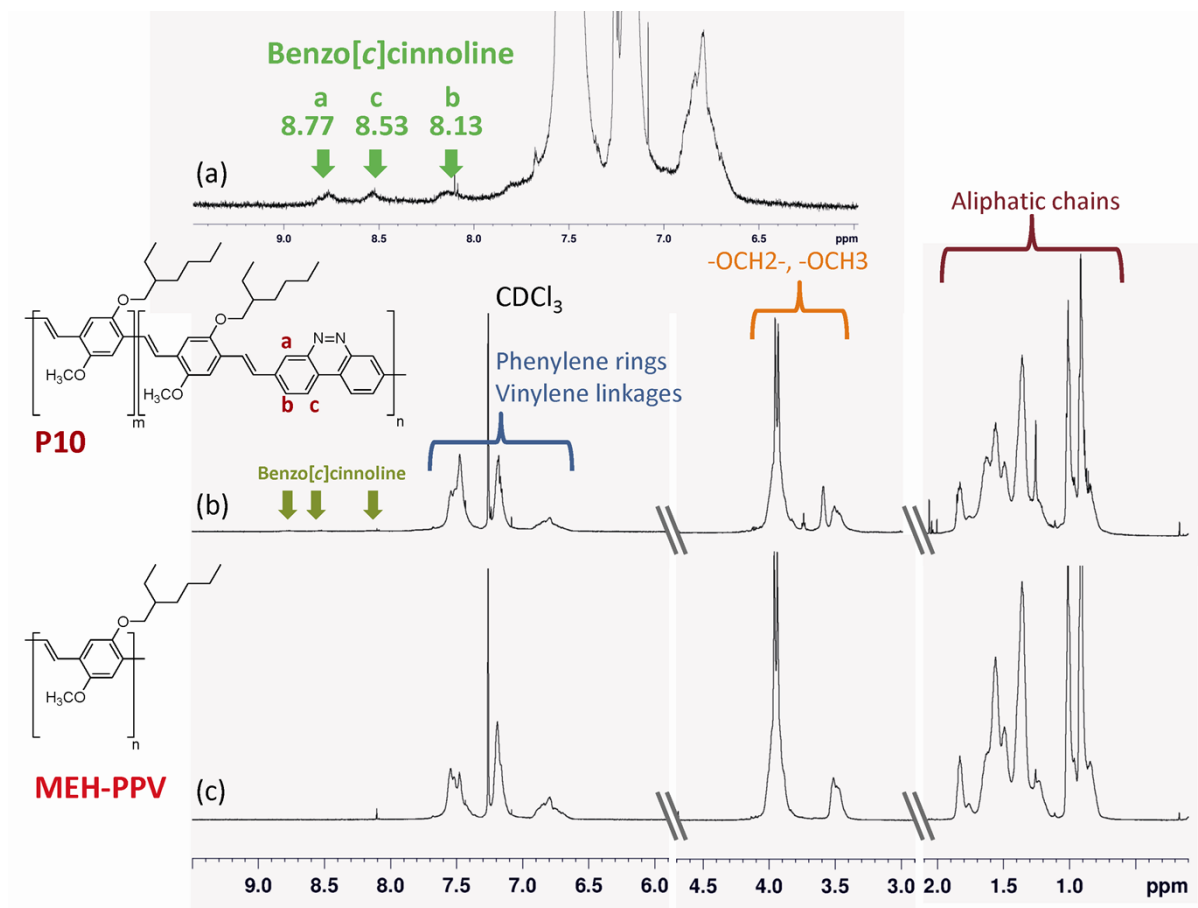


Fig. S2  $^1\text{H}$  NMR spectra of **P10** (a), (b) and MEH-PPV (c) in  $\text{CDCl}_3$ .

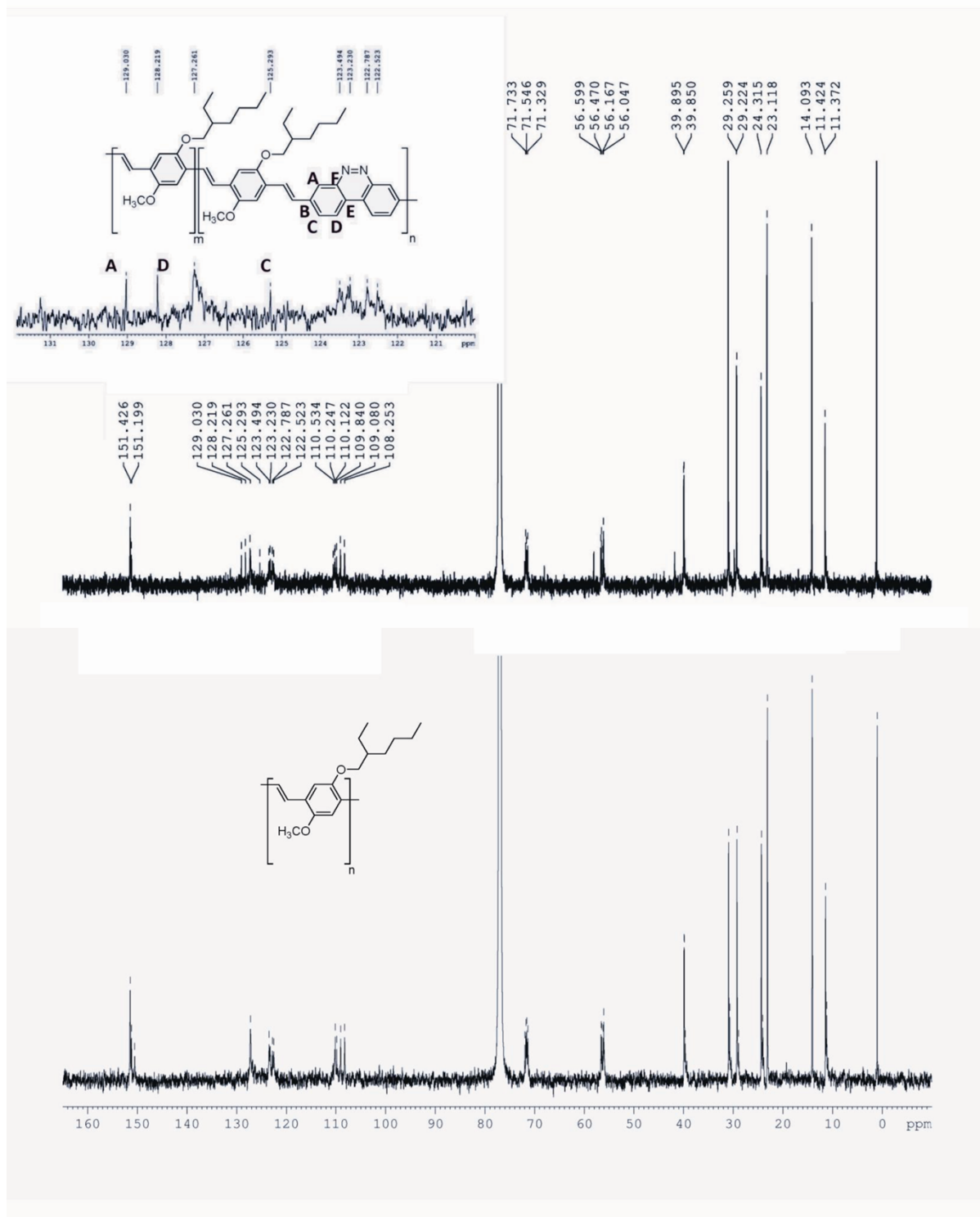


Fig. S3  $^{13}\text{C}$  NMR spectra of **P10** and MEH-PPV in  $\text{CDCl}_3$ .

## Redox Behavior Characterized by Cyclic Voltammetry

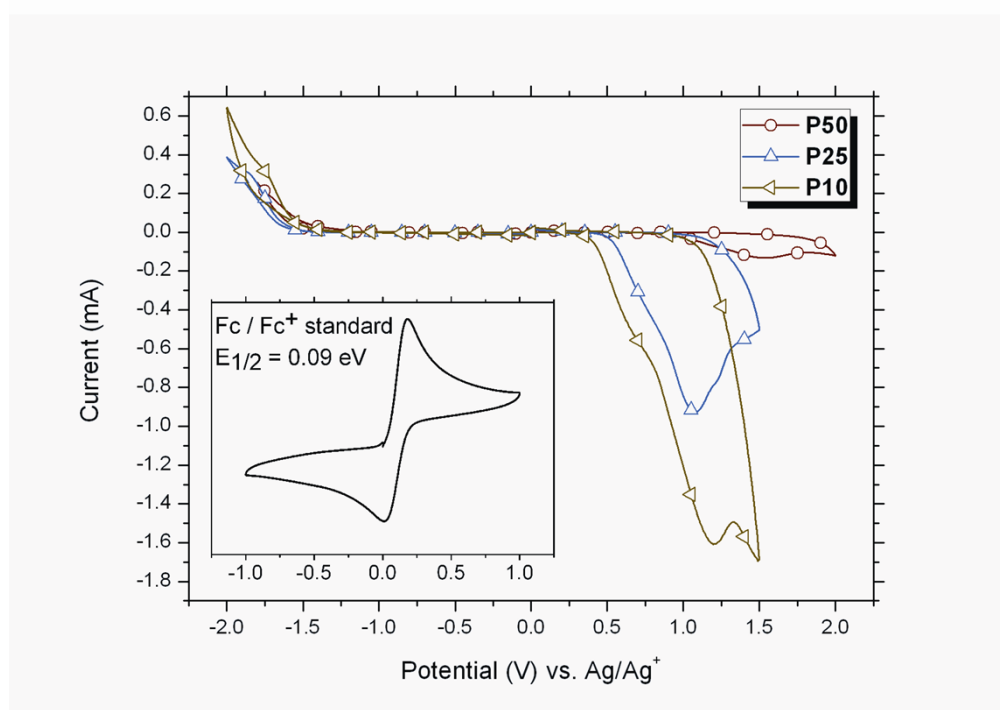


Fig. S4 Cyclic voltammograms of polymer films on an ITO-coated glass substrate in CH<sub>3</sub>CN containing 0.1M TBAP.

## Simulation methods

The theoretical calculations were carried out with the Maestro graphical interface of Schrodinger molecular modeling suite. (Maestro 9.4.047; Schrodinger, LLC: New York, [www.schrodinger.com](http://www.schrodinger.com)) The repeating units of MEH-PPV and **P50** were employed in the molecular simulation. The monomer structures were initially minimized using the OPLS\_2005 (MacroModel, Version 9.9.2; Schrodinger, LLC: New York, [www.schrodinger.com](http://www.schrodinger.com)) force field with a dielectric constant of 1.0. Full geometry optimization was then carried out using density functional theory (DFT) within Jaguar module of Schrodinger molecular modeling suite. (Jaguar 8.0; Schrodinger, LLC: New York, 2010) The hybrid functional of the DFT method B3LYP is combined with 6-31G\*\* basis set. SCF and convergence criteria were set at 5e-5 Hartree or RMS density matrix change of 5e-6,

whichever is met first. Single point electronic energy calculation on the optimized geometries were performed at the B3LYP/6-31G\*\* level of theory. All computation was executed on a 16 CPU Intel Xeon workstation running Red Hat Linux.